Supplementary information

Direct Ink Writing of Silver Nanowire-Based Flexible Temperature Sensors on Fabric for Wearable Thermal Monitoring

Jiajun Huang,[a] Shihao Yang,[a] Zhijie Ye,[a] Xinpeng Wang,[ab] Ziye Fang,[a] Qi Yu,[a] Bowen Li[a] and Yue-Hui Wang*[a]

[a] Zhongshan Institute, University of Electronic Science and Technology of China, Zhongshan 528402, China.

[b] Department of Material and Energy, University of Electronic Science and Technology of China, Chengdu 610054, China

* Corresponding author. E-mail address: wangzsedu@126.com (Yue-Hui Wang)

CAPTIONS

Figure S1 Graphic parameters of the PTC thermistor.

Figure S2 Viscosity of the AgNW-based conductive ink at shear rate of 50 s^{-1}.

Figure S3 Viscosity of the AgNW-based conductive ink at shear rates ranging from 0 to 150 s^{-1}.

Figure S4 UV-visible absorption spectra of the AgNW-based conductive ink and pristine AgNWs.

Figure S5 TG-DSC analysis of the AgNW-based conductive ink.

Figure S6 Sheet resistance values at different positions of the PTC thermistor.

Figure S7 Maximum allowable operating temperature of the AgNW-based flexible temperature sensor.

Figure S8 Microstructure of the copper wire before and after oxidation.

Figure S9 Volt-ampere characteristics curve of the AgNW-based flexible temperature sensor.

Figure S10 Comparison of the AgNW-based flexible temperature sensor with currently reported sensors.

Table S1 Comparison of the AgNW-based flexible temperature sensor with currently reported sensors.

FIGURES

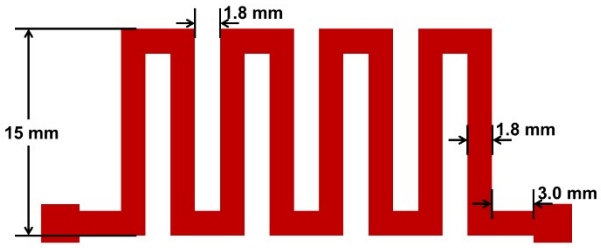

Figure S1 Graphic parameters of the PTC thermistor.

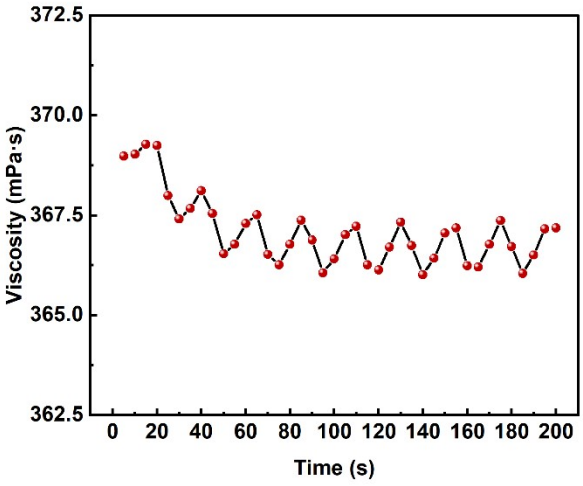

Figure S2 Viscosity of the AgNW-based conductive ink at shear rate of 50 s^{-1}.

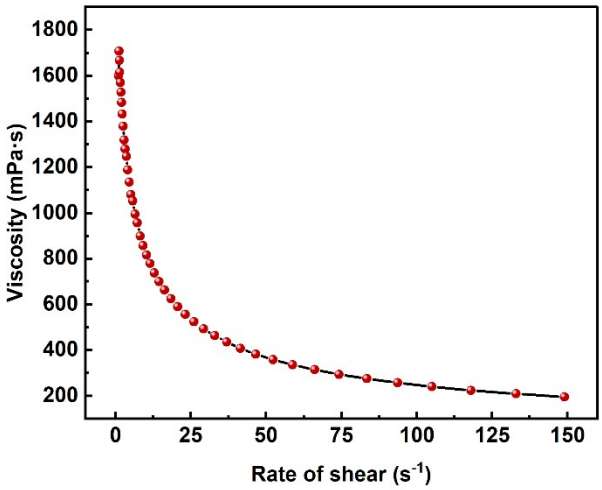

Figure S3 Viscosity of the AgNW-based conductive ink at shear rates ranging from 0 to 150 s^{-1}.

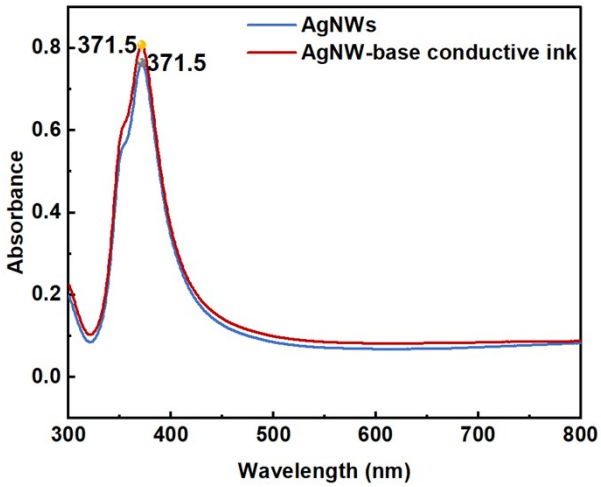

Figure S4 UV-visible absorption spectra of the AgNW-based conductive ink and pristine AgNWs.

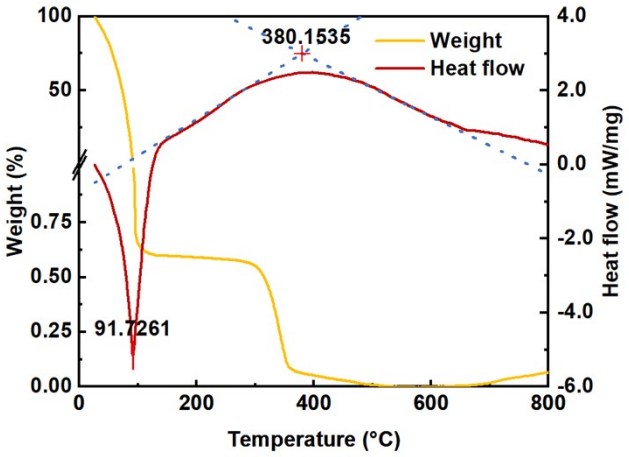

Figure S5 TG-DSC analysis of the AgNW-based conductive ink.

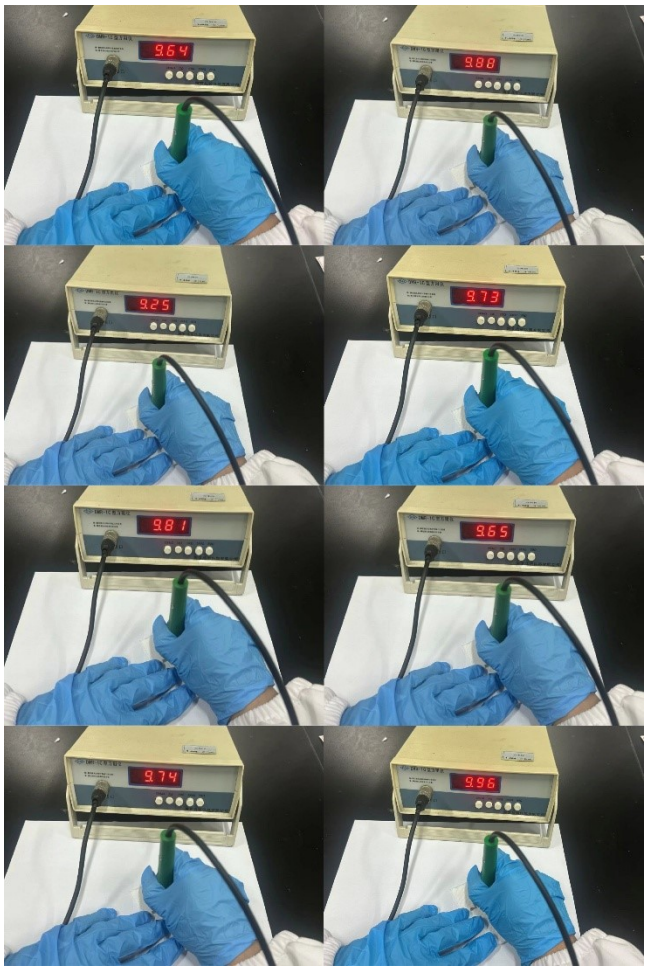

Figure S6 Sheet resistance values at different positions of the PTC thermistor.

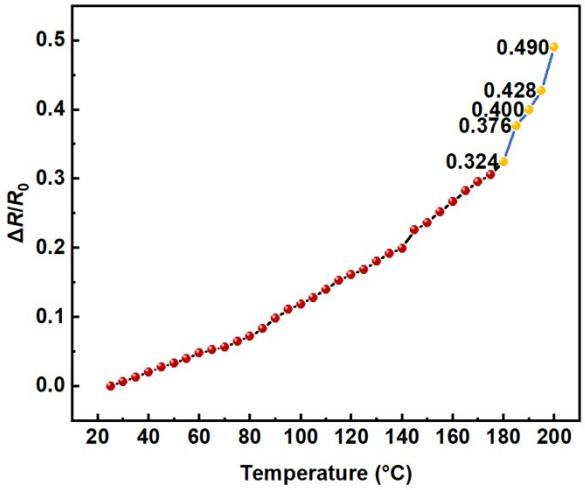

Figure S7 Maximum allowable operating temperature of the AgNW-based flexible temperature sensor.

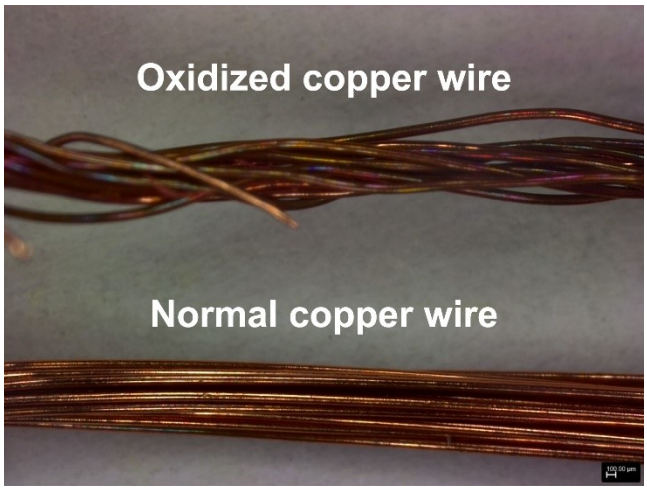

Figure S8 Microstructure of the copper wire before and after oxidation.

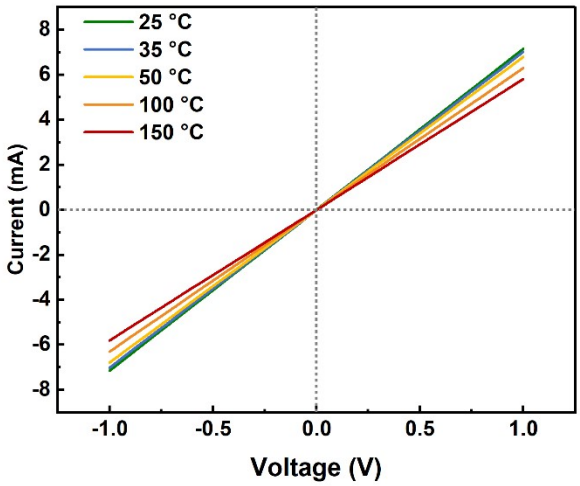

Figure S9 Volt-ampere characteristics curve of the AgNW-based flexible temperature sensor.

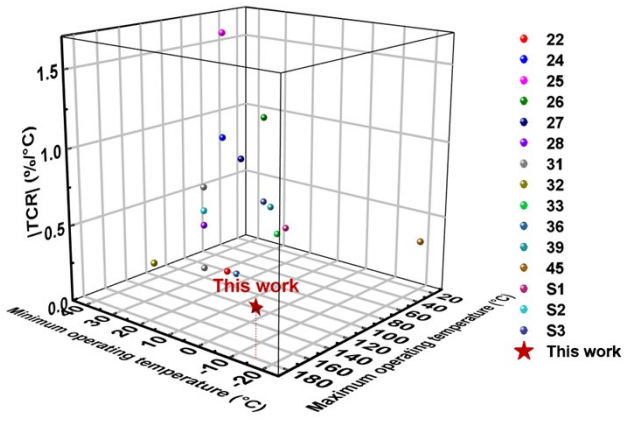

Figure S10 Comparison of the AgNW-based flexible temperature sensor with currently reported sensors.

TABLES

Table S1 Comparison of the AgNW-based flexible temperature sensor with currently reported sensors.

Temperature-sensitive material	Flexible substrate	*TCR* (%/°C)	Temperature range (°C)	Responds time (s)	Linearity	Reference
CNTs	PDMS	-0.046[#] (0.55 Ω/°C, ~1175 Ω)	25–90	--	Linear	[22]
MWCNT/CB	PVA/Gly organohydrogel	-0.935	30–80	--	Linear (R^2 = 0.99)	[24]
CNTs	XSBR	-1.636	30–80	--	Nonlinear	[25]
MWCNTs	Fabric	-1.04	25–50	--	Nonlinear	[26]
graphene	PDMS	0.8	25–75	1.32–3.91	Linear	[27]
rGO	PET	0.37	30–100	0.196–0.274	Linear (R^2 = 0.996)	[28]
rGO	PET	0.6345	30–100	1.2	Linear	[31]
MWCNTs	PET	0.068	30–100	--	Linear	[31]
AgNPs	NP films	0.235 ± 0.0176	30–150	--	Linear	[32]
AgNWs	PIC hydrogels	0.24	20–50	--	Linear	[33]
Cr/Au	PI/PDMS	0.00104	25–80	1	Linear (R^2 = 0.999)	[36]
Ag	TPU-coated polyester fabric	0.262	25–42	--	Linear (R^2 = 0.9955)	[39]
AgNWs	CPI	0.33	-20–20	--	Linear	[45]
Ti/Au	PI/Polyester yarns	0.258	20–40	2.4 ± 0.5	Linear	[60]
MWCNTs	Fabric	0.471	30–100	--	Linear (R^2 = 0.9806)	[61]
PPy	PP nonwoven fabric	0.447	25–50	50	Linear (R^2 = 0.99374)	[62]
AgNWs	Fabric	0.229 (-15–20 °C) 0.115 (20–70 °C) 0.200 (70–135 °C) 0.315 (135–150 °C)	-15–180	7–102	Linear (R^2 > 0.988)	This work

[#] Denotes data processed through a formula using other relevant data from the references.